Smartphone Video Guidance Sensor for Small Satellites

Christopher Becker, Richard Howard, John Rakoczy
NASA Marshall Space Flight Center
Mail Stop EV42, Huntsville, AL 35812; 256-544-0114
christopher.m.becker@nasa.gov

ABSTRACT

The Smartphone Video Guidance Sensor (SVGS) is a miniature, self-contained autonomous rendezvous and docking sensor developed using a commercial off the shelf Android-based smartphone. SVGS enables proximity operations and formation flying capabilities for small satellite platforms. SVGS determines the relative position and orientation between two cubesats or other small satellites. The sensor performs pose estimation by illuminating and capturing an image of retroreflective targets mounted in a known pattern on the target spacecraft using the smartphone camera and flash. The resulting image is then processed using a modification of algorithms originally developed at NASA Marshall Space Flight Center for the Advanced Video Guidance Sensor (AVGS), which successfully flew on the Demonstration for Autonomous Rendezvous Technology (DART) and Orbital Express missions. These algorithms use simple geometric photogrammetry techniques to determine the six-degree of freedom state of one spacecraft relative to the other. All image processing and computational requirements are performed using the smartphone's processing capabilities, and the resulting calculated relative state is then provided to the host spacecraft's other guidance, navigation, and control subsystems.

INTRODUCTION

The Smartphone Video Guidance Sensor is part of ongoing efforts at NASA Marshall Space Flight Center (MSFC) to enhance and demonstrate the formation flying and proximity operations capabilities of cubesats. Initial development of SVGS began in Fiscal Year 2013, and effort is continuing in Fiscal Year 2014 to increase SVGS functionality and to integrate SVGS onboard a MSFC-developed 6U cubesat for a proximity operations demonstration on the flat floor of the MSFC Flight Robotics Laboratory (FRL) later this year.

Android smartphones are currently on orbit onboard NASA Ames Research Center's PhoneSats, two PhoneSat 1.0 spacecraft using the HTC Nexus One and one 2.0 spacecraft with a Samsung Nexus S, and SSTL's STRaND-1 (Nexus One). Through these ongoing projects, the suitability of COTS Android devices in orbit is being demonstrated.

SVGS Background And Concept Of Operations

The Smartphone Video Guidance Sensor is a low mass, low volume, and low cost implementation of the Marshall Space Flight Center (MSFC) developed Advanced Video Guidance Sensor (AVGS) using commercial off the shelf (COTS) hardware. The SVGS is being designed specifically for application on cubesats and other small satellites to enable autonomous rendezvous and capture (AR&C) and formation flying. AVGS is an optical sensor that calculates the relative range and attitude (6-DOF state) between two spacecraft. AVGS was flown on the Demonstration of Autonomous Rendezvous Technology (DART) and Orbital Express demonstration missions in 2005 and 2007 respectively.

The basic concept behind the AVGS sensor is to use a light source to illuminate a known pattern of retroreflective targets on a target spacecraft. An image is then captured of the illuminated targets, and using simple geometric techniques, the 6-DOF state is extracted from the two dimensional image. While AVGS used a laser as its illumination source and a high quality CMOS sensor to capture the images, SVGS uses the camera and flash on a COTS Android-based smartphone.

The SVGS software was developed as an Android application and deployed on several COTS Android smartphones from different manufacturers during the prototype development process. The complete state calculation process including image capture, image processing, and relative state derivation is performed on the Android device. The SVGS concept of operations is illustrated in Figure 1. First retroreflective targets mounted on the target spacecraft are illuminated using the smartphone camera's flash. An image of the targets is then captured using the camera. This image is processed onboard the smartphone and the 6-DOF relative state calculated. The computed state can then be consumed by other applications on the smartphone or passed from the phone to the other avionics onboard

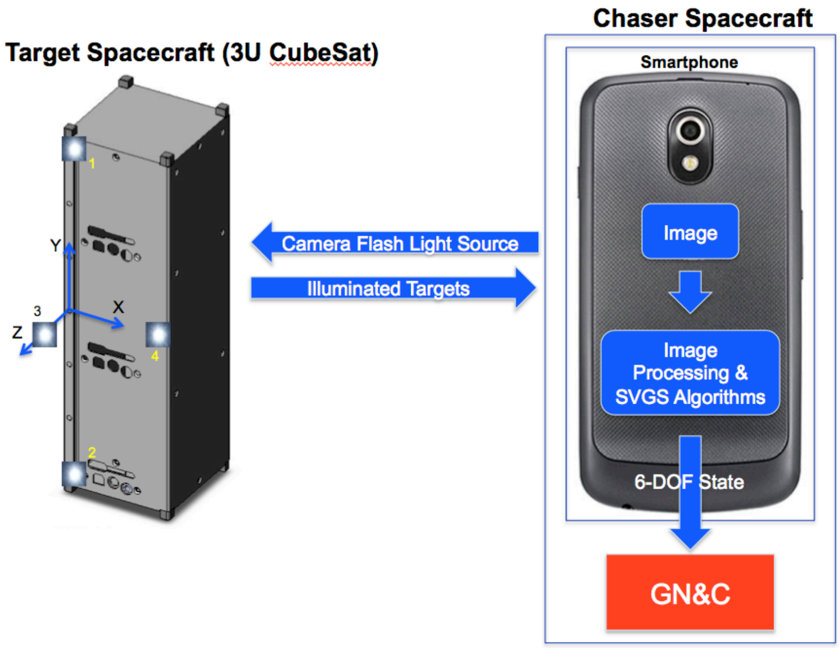

Figure 1: SVGS Concept of Operations

a small satellite as input data for the guidance, navigation, and control functions.

Target Pattern And Coordinate System

The target pattern used for SVGS testing is a modified version of the AVGS target pattern. The retroreflective targets are shown and numbered on the 3U cubesat mockup in Figure 1. Targets 1, 2, and 4 are mounted coplanar at the extreme edges of the long face of the 3U cubesat, and target 3 is mounted on a boom extending out of the face of the cubesat. By placing target 3 out of plane of the other three targets, the accuracy of relative attitude calculations is increased.

The SVGS target spacecraft coordinate system is defined as follows:

-The origin of the coordinate system is at the base of the target 3 boom.
-The y-axis points along the direction from target 2 to target 1.
-The z-axis points from the origin towards target 3.
-And the x-axis completes the right-handed triad.

The 6-DOF relative state outputted from the SVGS is calculated with respect to a coordinate system with the same orientation as above but with the origin located at the center of the image plane formed by the smartphone camera.

Table 1: Target Coordinates

Target	X (cm)	Y (cm)	Z (cm)
1	0	13.75	0
2	0	-13.75	0
3	0	0	5.0
4	8.75	0	0

For SVGS testing, the target spacecraft was represented by a Thorlabs MS12B/M mini optical breadboard. The targets were retroreflective corner cubes mounted on the breadboard at the coordinate locations shown in Table 1. This configuration was chosen to mimic possible mounting locations on a 3U cubesat.

SYSTEM DESCRIPTION

Collinearity Equations

AVGS uses the Inverse Perspective algorithm[1] to calculate the 6-DOF relative state between the target and chase vehicles. SVGS however uses photogrammetry techniques and an adaption of the collinearity equations[2] developed by Rakoczy[3] to solve for the desired state vector. If a thin lens camera system images the point "A" shown in Figure 2, all light rays leaving "A" and entering the camera will be focused at point "L", which is called the perspective center, and then an image of point "A" will be formed on the image plane represented in the figure as point "a".

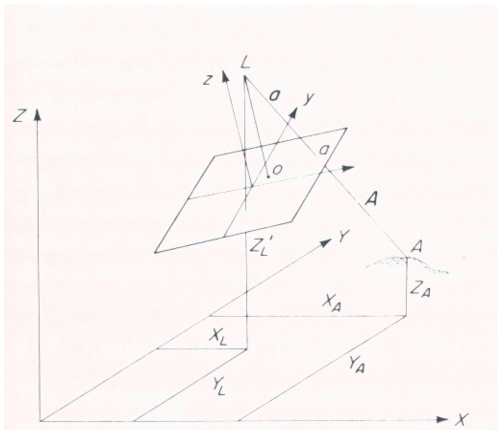

Figure 2: Object and Camera Frame Geometry[2]

Figure 2 also shows two coordinate frames: the object (or target) frame which is shown by the axes labeled with upper case letters X, Y, and Z, and the image (or chase) frame which is represented by the lower case letters x, y, and z.

A vector from the perspective center to point "A" can be defined in the object frame as in the following equation.

$$v_A = \begin{bmatrix} X_A - X_L \\ Y_A - Y_L \\ Z_A - Z_L \end{bmatrix} \quad (1)$$

Similarly a vector can be defined to point "a" from the perspective center as below.

$$v_a = \begin{bmatrix} x_a - x_0 \\ y_a - y_0 \\ -f \end{bmatrix} \quad (2)$$

These two vectors are related by the following equation where k is a scaling factor and M is a rotation matrix representing an x, y, z rotation sequence transforming the object frame to the image frame.

$$v_a = kMv_A \quad (3)$$

Dropping the "a" and "A" subscripts and solving for the image frame coordinates x, y, and z of point "a" and then dividing by the equation for z to eliminate the scaling factor k yields the following two equations labeled F_x and F_y. The m_{ij} values are elements of the direction cosine matrix M.

$$x = f\frac{m_{11}(X - X_L) + m_{12}(Y - Y_L) + m_{13}(Z - Z_L)}{m_{31}(X - X_L) + m_{32}(Y - Y_L) + m_{33}(Z - Z_L)} + x_0 = F_x \quad (4)$$

$$y = f\frac{m_{21}(X - X_L) + m_{22}(Y - Y_L) + m_{23}(Z - Z_L)}{m_{31}(X - X_L) + m_{32}(Y - Y_L) + m_{33}(Z - Z_L)} + y_0 = F_y \quad (5)$$

The relative 6-DOF state vector that needs to be solved for is V, defined below where ϕ, θ, and ψ represent the x, y, z rotation angles respectively.

$$V = \begin{bmatrix} X_L \\ Y_L \\ Z_L \\ \phi \\ \theta \\ \psi \end{bmatrix} \quad (6)$$

Linearizing F_x and F_y using a Taylor series expansion truncated after the second term yields the following two equations,

$$x = F_x(V_0) + \frac{\partial F_x}{\partial V}\Delta V + \varepsilon_x \quad (7)$$

$$y = F_y(V_0) + \frac{\partial F_y}{\partial V}\Delta V + \varepsilon_y \quad (8)$$

where V_0 is an initial guess for the state vector, ΔV is the difference between this guess and the actual state vector as seen below,

$$\Delta V = V - V_0 \quad (9)$$

and ε_x and ε_y are the x and y error due to the Taylor series approximation.

Each of the 4 targets in the SVGS target pattern will have a corresponding set of these two equations. Compiling these 8 equations and representing them in matrix form, using the following definitions,

$$Y = \begin{bmatrix} x_1 \\ y_1 \\ . \\ . \\ x_4 \\ y_4 \end{bmatrix} \quad Y_0 = \begin{bmatrix} F_{x1} \\ F_{y1} \\ . \\ . \\ F_{x4} \\ F_{y4} \end{bmatrix} \quad H = \begin{bmatrix} \frac{\partial F_{x1}}{\partial V} \\ \frac{\partial F_{y1}}{\partial V} \\ . \\ . \\ \frac{\partial F_{x4}}{\partial V} \\ \frac{\partial F_{y4}}{\partial V} \end{bmatrix} \quad (10)$$

yields the following.

$$Y = Y_0 + HV + \varepsilon \quad (11)$$

This equation is solved for the V that minimizes the square of the residuals ε. This value is then added to the intial estimate of V to get the updated state vector. The process is iterated until the residuals are sufficiently small yielding the final estimate of the 6-DOF state vector V.

SVGS Collinearity Formulation

For SVGS, the general form of the collinearity equations described in the previous section is specialized to reflect the state vector formulation used by AVGS. AVGS sensor measurements used angle pairs, azimuth and elevation, measured in the image frame to define the location of each retroreflective target in the image. Azimuth and elevation are measured with respect to a vector to the perspective center and the target locations in the captured image. Azimuth, Az, is defined in Equation 12, and elevation, El, is defined in Equation 13[3]. Equations 12 and 13 then replace Equations 4 and 5 in the previous derivation.

$$Az = \tan^{-1}\left(\frac{x - x_0}{f}\right) \tag{12}$$

$$El = \sin^{-1}\left(\frac{y - y_0}{\sqrt{(x - x_0)^2 + (y - y_0)^2 + f^2}}\right) \tag{13}$$

SVGS Algorithms

The SVGS calculation process begins with the illumination by the smartphone camera flash of the target pattern on the target spacecraft. An image of the illuminated targets is then captured and processed. The image is first converted to a binary image using a specified brightness threshold value. Blob extraction is then performed on the binary image to find all bright spot locations. Location and size and shape characteristics of the blobs are captured.

Depending on if there are any other objects in the field of view that may generate bright background noise spots, the number of blobs may exceed the number of targets. To account for any noise and to properly identify which target is which, a subset of four blobs is selected from all identified and some basic geometric alignment checks derived from the known orientation of the targets are applied. This process is iterated until the four targets have been found and properly labeled.

The target centroids are then fed into the state determination algorithms. Using the collinearity equation formulation, the relative state is determined using a simple least squares process. The SVGS process is illustrated in Figure 3.

Test Setup

SVGS testing was performed in the MSFC Flight Robotics Laboratory. The target pattern setup and SVGS were mounted on the Newmark Systems rotary and translation tables in the FRL. The SVGS sensor was mounted on the Sensor Mount (Figure 4), a 3-axis rotation motorized gimbal mounted on a 1-axis motorized translation stage. The 3-axis rotation gimbal allows for ±25 degrees roll and pitch and ±45 degrees yaw. The translation stage allows for ±15 cm precision movement on an axis aligned in the direction between the Sensor and Target Mounts. In addition to the motorized 1-axis motion provided by the stage, the entire Sensor Mount setup is mounted on a wheeled cart that can be moved along a rail mounted on the floor that runs the full length of the FRL.

The mini optical breadboard with the desired target pattern of retroreflectors is mounted on the Target Mount, a 2-axis rotation stage which allows for motion along the SVGS-defined roll and pitch axes. For the SVGS testing described in this document, the Target Mount was left in a static position and alignment. All relative motion was performed using the Sensor Mount.

Figure 3: SVGS Algorithm Flow

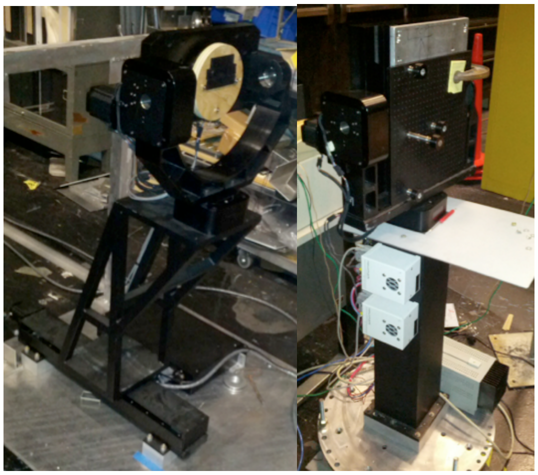

Figure 4: Sensor Mount (left), Target Mount (right)

The motion of the motorized elements of the Sensor and Target Mounts is controlled by stepper motors using a motion controller. Using the provided software APIs, the stage motions were controlled and integrated with the SVGS test script to allow for completely autonomous testing sequences with minimal operator input. In addition to the fine attitude and position truth data provided by the Newmark rotary and linear stages, a handheld (insert model number) laser rangefinder with (insert accuracy) accuracy was used for gross range information between the Sensor and Target Mounts.

Figure 5: 12.7 mm Diameter Corner Cube

For the test results presented in the following section, testing was performed using two stock Android smartphones from two different manufacturers (HTC Amaze 4G and Samsung Galaxy Nexus) running Android 4.0+. For this testing sequence, the retroreflective targets used were Edmund Optics Mounted N-BK7 12.7 mm diameter corner cubes shown in Figure 5. The corner cubes were mounted as shown in Figure 1 and Table 1. Because the corner cubes are so effective at reflecting a large concentration of light received back in the direction of the emanating light source, they were ideal for allowing large ranges between the target and the SVGS.

Prior to testing, a succession of images was captured using each phone from a known range to the targets. By iterating between each successive image, a rough approximation of each camera's focal length was calibrated. This value is required to calculate an accurate 6-DOF relative state.

TEST RESULTS

SVGS prototype testing results are documented in the following tables and figures. Table 2 and Table 3 show the mean error and standard deviation for each component of the 6-DOF state for the first smartphone platform tested (Amaze 4G), while Table 4 and Table 5 show the same data for second phone (Galaxy Nexus). Figures 6 through 9 show are error histograms for each component of the relative state for the Amaze 4G. Figures 10 through 13 are the error histograms for the Galaxy Nexus.

Because the camera and flash hardware on the two phones were different and manufacturers often make modifications to the basic Android operating system environment, Amaze 4G only provided effective state calculations up to about a 6.5 meter range. Beyond that distance, because of the particular software settings available on Amaze 4G and the relatively closely spaced retroreflectors in the 3U configuration, the four bright spots in the captured image from the retroreflectors merged into a single spot that prevented accurate centroiding of the retroreflector returns. Possible remedies for this issue could include replacing the corner cubes with reflectors with a lower return brightness or increasing the spacing between the reflectors. However an increase in the spacing would preclude use of this system on a 3U platform. The test results for Amaze 4G show a maximum error of 10 cm in position and 1.1 degrees in attitude.

The configuration of Galaxy Nexus allowed for considerably longer test ranges than Amaze 4G. The formal test procedure was repeated up to a range of 30 meters from the targets. This range was limited only by the configuration of the test lab. Spot testing was performed at longer ranges with successful state solutions computed at ranges approaching 40 meters. The Galaxy Nexus test data shows an increase in state error with an increase in total range, with a maximum state error of 1.53 meters in position and 3.0 degrees in attitude at 30 meters. The Z-axis, which is aligned along the camera boresight, shows a smaller position error than the X and Y components.

Table 2: Amaze 4G Relative State Mean Error

Range (m)	Position (m)			Attitude (deg)		
	X	Y	Z	Roll	Pitch	Yaw
1	0.07	0.03	0.02	1.0	0.9	0.3
2	0.07	0.04	0.01	0.9	0.6	0.3
3	0.06	0.05	0.03	0.7	0.5	0.3
4	0.07	0.06	0.04	0.5	0.4	0.3
6.5	0.05	0.10	0.07	1.1	0.5	0.7

Table 3: Amaze 4G Relative State Standard Deviation

Range (m)	Position (m)			Attitude (deg)		
	X	Y	Z	Roll	Pitch	Yaw
1	0.016	0.022	0.013	0.47	0.52	0.29
2	0.016	0.016	0.009	0.37	0.40	0.14
3	0.028	0.024	0.014	0.43	0.37	0.18
4	0.033	0.028	0.018	0.35	0.32	0.19
6.5	0.037	0.048	0.030	0.44	0.40	0.25

Table 4: Galaxy Nexus Relative State Mean Error

Range (m)	Position (m)			Attitude (deg)		
	X	Y	Z	Roll	Pitch	Yaw
5	0.05	0.08	0.07	0.6	0.9	2.0
10	0.10	0.16	0.13	0.7	1.0	1.8
15	0.26	0.30	0.18	0.9	1.2	1.9
20	0.41	0.50	0.23	1.3	1.6	2.0
30	1.12	1.53	0.47	2.2	3.0	1.2

Table 5: Galaxy Nexus Relative State Standard Deviation

Range (m)	Position (m)			Attitude (deg)		
	X	Y	Z	Roll	Pitch	Yaw
5	0.037	0.038	0.039	0.39	0.24	0.04
10	0.077	0.098	0.076	0.50	0.24	0.06
15	0.188	0.193	0.116	0.72	0.36	0.11
20	0.269	0.382	0.140	0.99	0.30	0.13
30	0.744	0.887	0.352	1.50	0.72	0.26

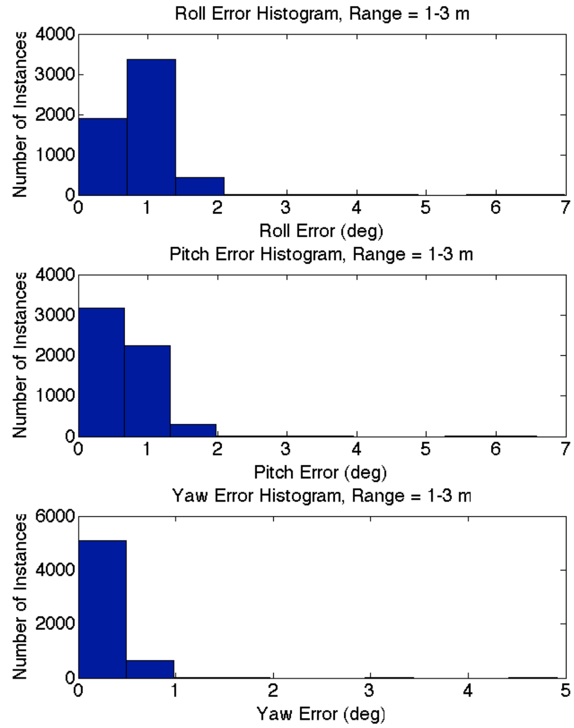

Figure 6: Amaze 4G - Position Error (1-3 m range)

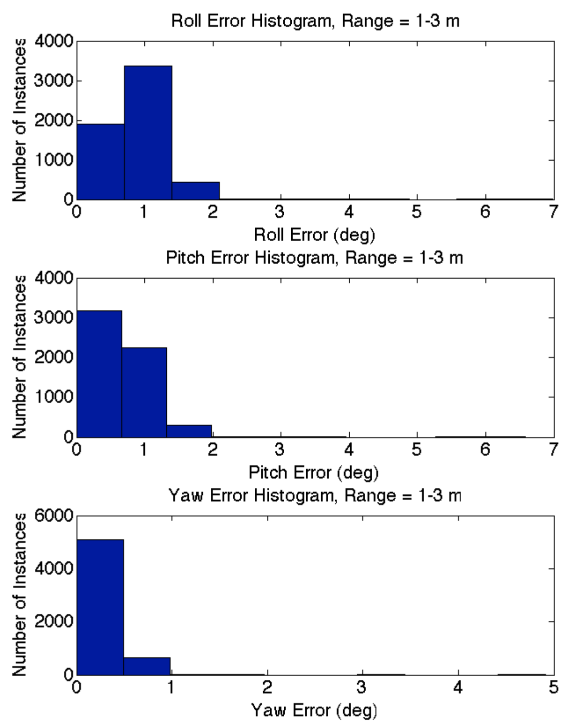

Figure 7: Amaze 4G - Attitude Error (1-3 m range)

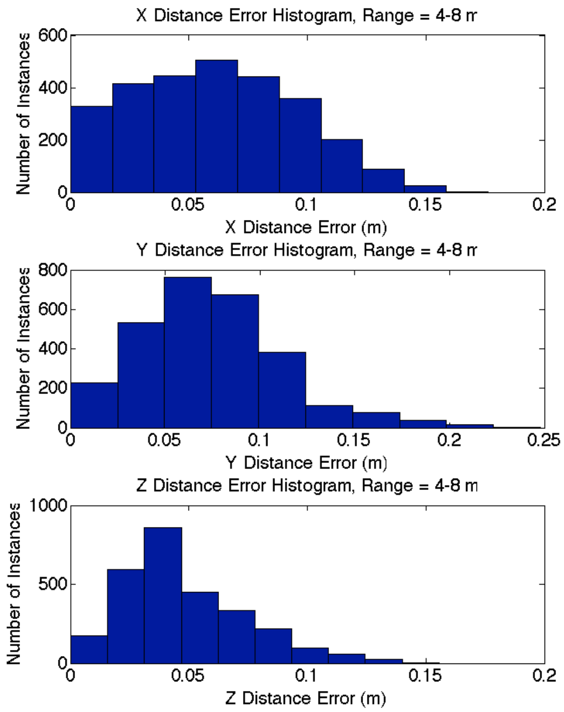

Figure 8: Amaze 4G - Position Error (4-8 m range)

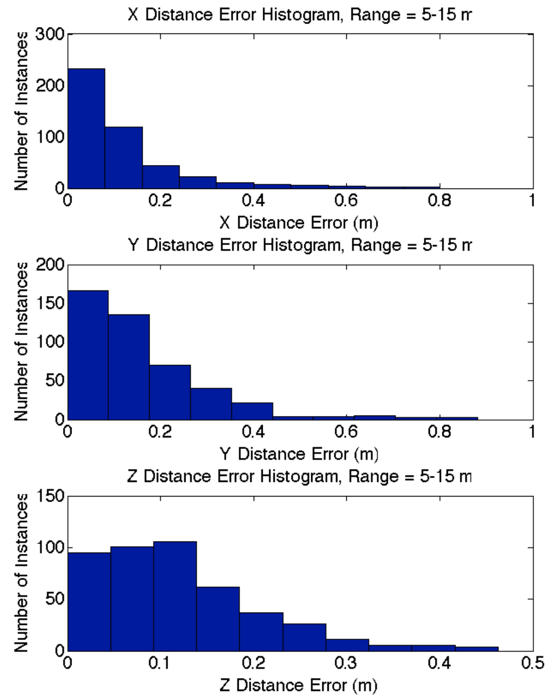

Figure 10: Galaxy Nexus - Position Error (5-15 m range)

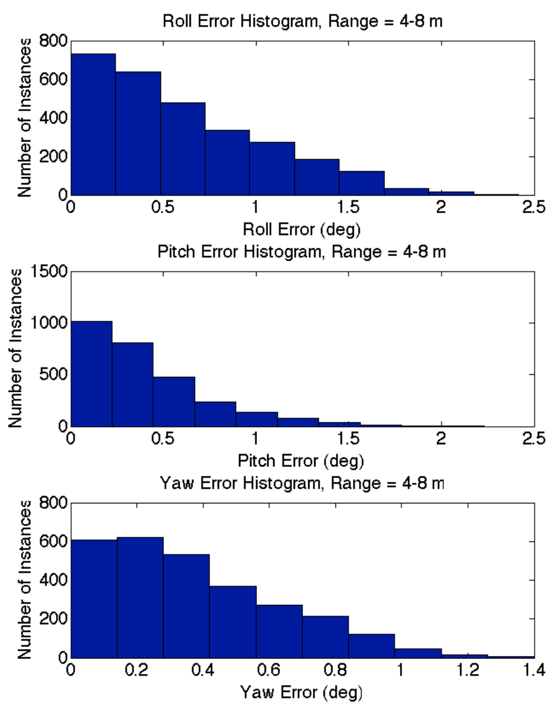

Figure 9: Amaze 4G - Attitude Error (4-8 m)

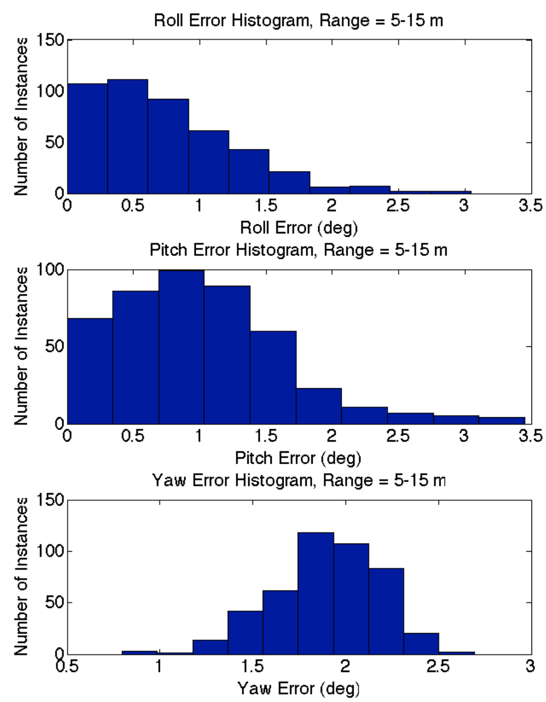

Figure 11: Galaxy Nexus - Attitude Error (5-15 m range)

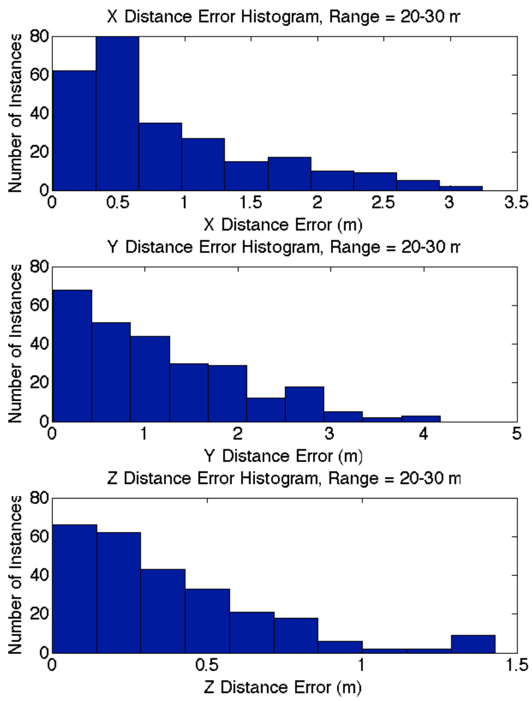

Figure 12: Galaxy Nexus - Position Error (20-30 m range)

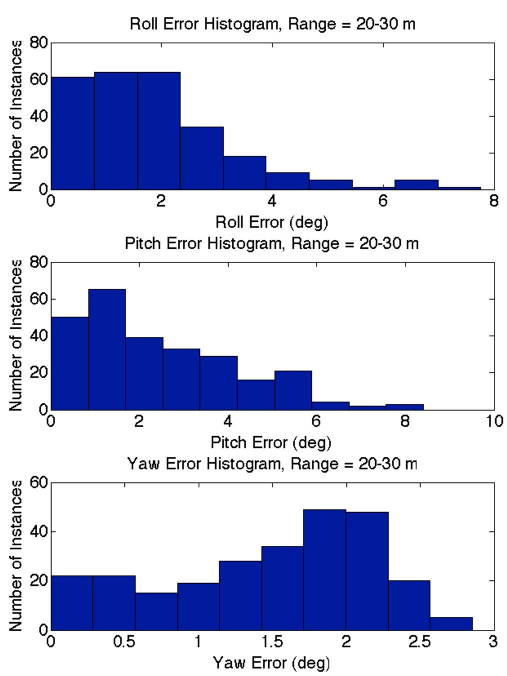

Figure 13: Galaxy Nexus - Attitude Error (20-30 m range)

CONCLUSIONS AND FUTURE WORK

Results from testing of the Smartphone Video Guidance Sensor prototype validate that an Android smartphone is a suitable platform for development of a low-cost, low-mass, commercial off the shelf based autonomous rendezvous and capture sensor for cubesat and other small satellite spacecraft.

Future planned development work of SVGS includes a project currently in progress in Fiscal Year 2013 to integrate the SVGS with the avionics of a cubesat and demonstrate proximity operations. The cubesat will be floated on an air bearing on the flat floor in the Flight Robotics Laboratory at MSFC and various approach techniques will be demonstrated using a micro-propulsion system onboard the cubesat and SVGS as the AR&C sensor providing relative state updates between the cubesat and a second "spacecraft". Other further improvements planned to increase the accuracy of the relative state solutions provided by SVGS include performing a more formal camera calibration process to calculate the intrinsic parameters of the smartphone cameras. Increased accuracy may also be achieved by improving the centroid calculation process performed on the captured images.

Smartphones also now commonly include other sensors such as accelerometers, gyroscopes, and magnetometers. Future development efforts of SVGS may include integrating these sensor measurements to improve and expand on the current SVGS relative state data. We also plan to perform vibration, thermal, and/or vacuum testing to raise the TRL of SVGS to prepare SVGS for a possible future flight opportunity.

References

1. Mullins, L., Heaton, A. and Lomas, J., "Advanced Video Guidance Sensor Inverse Perspective Algorithm," Marshall Space Flight Center, AL, December 2003.

2. Moffitt, F.H and Mikhail, E.M., Photogrammetry, Harper & Row Inc., New York, 1980.

3. Rakoczy, J., "Application of the Photogrammetric Collinearity Equations to the Orbital Express Advanced Video Guidance Sensor Six Degree-of-Freedom Solution," NASA MSFC internal memo #XD-31-(-05-004), Marshall Space Flight Center, AL, 31 March 2005.